Doubly excited autodissociating resonant states of positronium hydride

Yi Zhang,[1] Meng-Shan Wu,[1,*] Guo-An Yan,[2] Kalman Varga,[3] Zong-Chao Yan,[4,5] and Jun-Yi Zhang[5,†]

[1]*Center for Theoretical Physics, Hainan University, Haikou 570228, China*

[2]*School of Physics and Physical Engineering, Qufu Normal University, Qufu 273165, China*

[3]*Department of Physics and Astronomy, Vanderbilt University, Nashville, Tennessee 37235, USA*

[4]*Department of Physics, University of New Brunswick, Fredericton, New Brunswick, Canada E3B 5A3*

[5]*State Key Laboratory of Magnetic Resonance and Atomic and Molecular Physics, Wuhan Institute of Physics and Mathematics, Chinese Academy of Sciences, Wuhan 430071, China*

(Received 21 August 2023; accepted 30 October 2023; published 16 November 2023)

A doubly excited autodissociating resonant state in positronium hydride has been discovered, which is situated in a Rydberg series converging to the $H^-(2s^2) + e^+$ threshold. Previous research has noted a scarcity of such highly excited resonant states, particularly those with a doubly excited nature. The exploration of these states was made possible by employing a projection operator method supported by the stochastic variational method. Accurate calculations of the resonant positions and widths were performed using the complex coordinate rotation method with explicitly correlated Gaussians as basis functions. Our analysis has revealed the intrinsic structural characteristics of these highly excited states. The probability density distribution demonstrates that most resonant states of positronium hydride tend to favor either a $H^- + e^+$ or $Ps^- + H^+$ configuration. However, two doubly excited resonant states exhibit a unique characteristic involving both the $H^- + e^+$ and $Ps^- + H^+$ configurations. By integrating the probability density distribution with a quantum defect formula, highly excited resonances can be accurately assigned to either the $H^-(2s^2) + e^+$ or $Ps^-(1s^2) + H^+$ Rydberg series, thereby reducing discrepancies compared to earlier classifications.

DOI: 10.1103/PhysRevA.108.052813

I. INTRODUCTION

Positronium hydride (PsH), a binary system consisting of a hydrogen atom (H) and a positronium atom (Ps), can be envisaged as a negatively charged hydrogen ion (H^-) accompanied with a positron (e^+). The reaction of H^- with H and H_2 has been affirmed in interstellar clouds, with H^- recognized as a key influencer in the absorption of celestial radiation [1–3]. Concurrently, the positronium ion (Ps^-) manifests as a finite-life bound state, with PsH perceived as a Ps^- binding a proton (H^+). The annihilation of Ps^- culminates in the emission of γ rays at 511 keV, casting a significant imprint on stellar spectra [4,5]. The inception of PsH through positron-methane collisions was initially observed by Schrader *et al.* [6]. The PsH system involves two bound states: the ground state PsH ($1s^2\ ^1S^e$) [7–9] and an unnatural parity state PsH ($2p^2\ ^3P^e$) [10]. Additionally, numerous resonant states exist below the dissociation threshold within the PsH system. Recently, the spontaneous radiative dissociation of PsH beneath the Ps($2s$ or $2p$) + H($2s$ or $2p$) thresholds has been studied [11] by calculating the radiative transitions between resonant states and the second bound state, illuminating the absorption of astral light. Here, we aim to identify highly resonant states by particularly focusing on doubly excited states in Ps-H scattering. These resonances may be associated with optical transitions that involve excited states of both H and Ps.

Numerous investigations have been conducted regarding the resonances in the Ps-H scattering system [8,11–25]. Drachman employed an optical potential formalism to determine the energies associated with S-, P-, and D-wave resonances, which arise from the binding of a positron to H^- [13]. Yan and Ho [8,16–18] refined the analysis by utilizing the complex coordinate rotation (CCR) method along with Hylleraas basis sets, which facilitated the accurate determination of the resonant positions and widths of S-, P-, D-, F-, and G-wave resonances in PsH. Blackwood *et al.* [19] employed the coupled pseudostate approximation to identify high resonances. DiRienzi and Drachman [23] investigated the high-lying resonances within the Ps-H scattering system by employing the effective potential approach. Their study yielded predictions regarding the resonant energies of the Rydberg series converging to the $Ps^-(1s^2) + H^+$ threshold. Yan and Ho [24] later unveiled the resonant positions and widths of S-wave states in the $Ps^- + H^+$ Rydberg series, using the complex coordinate rotation method in Hylleraas basis sets. Additionally, they conducted computations for higher resonances, spanning from $1S$ to $8S$, which are the Rydberg series converging to the $H^-(1s^2) + e^-$ threshold [25].

To the best of our understanding, we have only been able to identify the Rydberg series of triply excited autodissociating resonant states in PsH, which converge towards the $H^-(2s^2) + e^+$ threshold. However, the identification of the simplest doubly excited autodissociating states still remains unknown [14].

*mswu@hainanu.edu.cn

†jzhang@apm.ac.cn

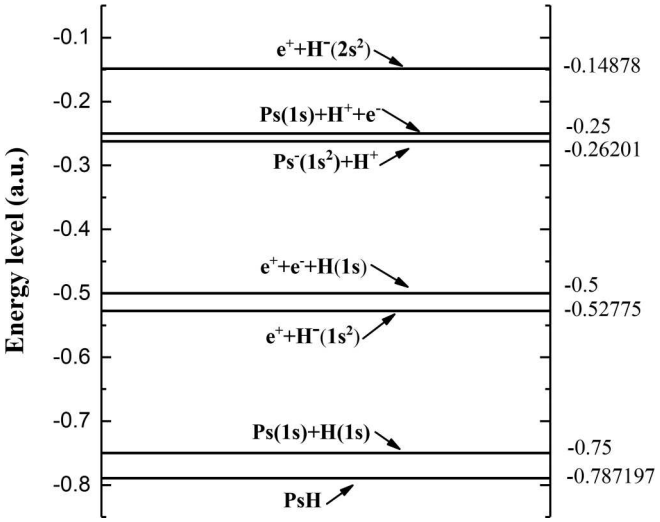

FIG. 1. Energy levels of the Ps-H system, in atomic units.

Furthermore, the energy level of the $H^-(2s^2) + e^-$ threshold is closely situated to the $Ps^-(1s^2) + H^+$ threshold, as depicted in Fig. 1. This suggests the possible existence of a doubly excited state in the $H^-(2s^2) + e^+$ Rydberg series, which shares a resonant position adjacent to a resonant state in the $Ps^-\ (1s^2) + H^+$ Rydberg series. In this paper, we investigate highly resonant states, particularly the doubly excited states, in Ps-H using a combination of a projection operator method and the stochastic variational method (SVM) [26–29]. The resonant positions and widths are refined using the complex coordinate rotation method in conjunction with explicitly correlated Gaussian (ECG) basis sets. These resonant states can be classified as Rydberg series, which converge towards the thresholds of $H^-(2s^2) + e^+$ or $Ps^-\ (1s^2) + H^+$.

The paper is organized as follows: Sec. II provides an overview of the projection operator method based on SVM that is employed for analyzing resonances in the PsH system. In Sec. III A, we present calculations for the resonant states (S-, P-, and D-wave resonances) situated below the $H^-(1s^2) + e^+$ threshold, and compare our findings with previous results. In Sec. III B, we investigate the highly excited S-wave resonant states within the Rydberg series converging to either the $H^-(2s^2) + e^+$ or $Ps(1s^2)^- + H^+$ threshold. Finally, we provide a summary in Sec. IV. Unless otherwise specified, atomic units are used throughout.

II. THEORETICAL METHOD

The SVM-based projection operator method has been proven to be highly effective in investigating resonant states across a wide range of systems [30–32]. This method utilizes the orthogonalizing pseudoprojector (OPP) operator as a penalty function, which is added to the Hamiltonian. This inclusion is intended to exclude certain orbitals from the active space, thereby inducing autoionization of the system. The OPP method approximates the computation of $\hat{Q}\hat{H}\hat{Q}$, where $\hat{Q} = 1 - \hat{P}$ represents the projection operator, and $\hat{P} = |\phi(\boldsymbol{r})\rangle\langle\phi(\boldsymbol{r})|$ with $\phi(\boldsymbol{r})$ being the orbital to be projected out. The energies obtained through the OPP method converge to those obtained by diagonalizing the $\hat{Q}\hat{H}\hat{Q}$ Hamiltonian.

In this paper, the OPP method is employed to examine the resonant states in the PsH system. To approximate the $\hat{Q}\hat{H}\hat{Q}$ Hamiltonian, the PsH Hamiltonian supplemented with the OPP operator is utilized. The modified Schrödinger equation for the PsH system can be written as follows:

$$(\hat{H} + \lambda\hat{P})\Psi = E_{\rm OPP}\Psi. \tag{1}$$

Assuming an infinite proton mass and considering the proton as the reference point in our coordinate system, we can express the nonrelativistic Hamiltonian as

$$\hat{H} = \hat{T} + \hat{V}, \tag{2}$$

where the kinetic-energy operator is

$$\hat{T} = -\frac{1}{2}\sum_{i=1}^{3}\nabla_{\mathbf{r}_i}^2, \tag{3}$$

and the potential-energy operator is

$$\hat{V} = -\frac{1}{r_1} - \frac{1}{r_2} + \frac{1}{r_3} + \frac{1}{r_{12}} - \frac{1}{r_{13}} - \frac{1}{r_{23}}, \tag{4}$$

with indices 1 and 2 being for the two electrons and index 3 being for the positron. In this paper, the parameter λ in Eq. (1) is 10^5 a.u., which is considerably greater than the values used in previous calculations [27,33–36], ensuring that the expected value of the OPP operator $\lambda\langle\hat{P}\rangle$ remains on the order of 10^{-8} a.u.

In this paper, an ECG basis is used to expand the wave function of the PsH system. This approach allows for an accurate representation of the correlations between charged particles [28,29,37,38]. The specific ECG basis functions used here have the form

$$\Phi_n(\mathbf{r}, s) = |\boldsymbol{\nu}|^{2K+L}\exp\left(-\tfrac{1}{2}\mathbf{r}^T A^{(n)}\mathbf{r}\right)Y_{LM}(\boldsymbol{\nu})\chi(s), \tag{5}$$

where L is the total orbital angular momentum of the system, $\mathbf{r}^T = (\mathbf{r}_1, \mathbf{r}_2, \mathbf{r}_3)$, and $\boldsymbol{\nu} = \mathbf{u}^T\mathbf{r}$ with $\mathbf{u}^T = (u_1, u_2, u_3)$ a global vector associated with L. Additionally, $\chi(s)$ represents the total electronic spin, which is set to be the spin-singlet state for all calculations in this paper. The independent parameters $A_{ij}^{(n)}$, encapsulated in the $n \times n$ symmetric matrix $A^{(n)}$, are optimized through energy minimization using the stochastic variational method. To account for the increasing number of nodes in excited states, the preexponential factor $|\boldsymbol{\nu}|^{2K+L}$ is introduced, where K is an integer.

The modified Schrödinger equation Eq. (1) can be solved to obtain the OPP energy $E_{\rm OPP}$. This energy converges towards the actual resonance position E_R but with a small deviation [34,39]:

$$E_R = E_{\rm OPP} + \Delta_Q, \tag{6}$$

where the shift Δ_Q is a small positive value that arises from the original $\hat{Q}\hat{H}\hat{Q}$ operator. To eliminate this shift and obtain precise values for the resonance position E_R and width Γ, we apply the CCR method [40,41] in conjunction with the ECG basis.

The CCR method utilizes a transformation $r \to re^{i\theta}$ to achieve both square integrability and expandability of the resonant wave function in terms of a basis set. This transformation leads to the definition of the transformed Hamiltonian,

TABLE I. Expectation values of various structural properties for the lowest resonant states of S, P, and D symmetries in Rydberg series converging to the $H^-(1s^2)+e^+$ threshold. The corresponding expectation values for the $H^-(1s^2)$ system are also listed as a comparison. Values are given in atomic units.

	$E_{\rm OPP}$	$\langle r_1\rangle$	$\langle r_3\rangle$	$\langle r_{13}\rangle$	$\langle r_1^2\rangle$	$\langle r_3^2\rangle$	$\langle r_{13}^2\rangle$	$\langle\delta(\mathbf{r}_1)\rangle$	$10^4\langle\delta(\mathbf{r}_{13})\rangle$
$S^{\rm I}(1)$	−0.6114403	2.44651	9.05956	9.17613	9.2315	91.720	96.031	0.1718	7.51
$P^{\rm I}(1)$	−0.5975741	2.56849	10.2113	10.2723	10.447	116.18	119.92	0.1677	6.30
$D^{\rm I}(1)$	−0.5777915	2.79253	12.7893	12.7012	13.253	181.63	182.75	0.1642	4.17
$H^-(1s^2)$	−0.5277510	2.71018			11.914			0.1644	

denoted as $\hat{H}_\theta$, which incorporates Coulombic interactions:

$$\hat{H}_\theta = \exp(-2i\theta)\hat{T} + \exp(-i\theta)\hat{V}. \tag{7}$$

To determine the resonance position E_R and width Γ, the complex eigenvalue problem for $\hat{H}_\theta$ is solved and the corresponding eigenvalue can be expressed in the form

$$E^c = E_R - \frac{i\Gamma}{2}. \tag{8}$$

By adjusting the rotation angle θ and minimizing the energy change with varying θ, the resonant state can be identified. To enhance accuracy, dilation parameters $\alpha = 0.99$, 1, and 1.01 are introduced [32,42,43]. The dilation is defined as the following transformation of all coordinates of the dynamical system: $r \to r\alpha$. Different dilation parameters are employed to establish a connection with the same resonant state.

III. RESULTS AND DISCUSSION

A. Resonant states in Rydberg series converging to the $H^-(1s^2)+e^+$ threshold

In this section, our objective is to identify the resonant states that are part of the Rydberg series converging to the threshold of $H^-(1s^2)+e^+$, while exhibiting S, P, and D symmetries. To achieve this, we utilized the OPP method, which involves excluding the Ps($1s$) orbital. The OPP operator is defined as the sum of two wave functions representing the Ps($1s$) orbital. Subsequently, we diagonalize the modified PsH Hamiltonian in order to obtain the OPP basis, which is used to represent the resonant state. The OPP operator $\hat{P}$ is defined as

$$\hat{P} = |\phi_{\rm Ps}(\boldsymbol{r}_{13})\rangle\langle\phi_{\rm Ps}(\boldsymbol{r}_{13})| + |\phi_{\rm Ps}(\boldsymbol{r}_{23})\rangle\langle\phi_{\rm Ps}(\boldsymbol{r}_{23})|. \tag{9}$$

The Ps($1s$) wave function $\phi_{\rm Ps}(\boldsymbol{r}_{ij})$ is expanded using a linear combination of ten ECGs, with a resulting ground-state energy eigenvalue of −0.249 999 a.u.

In Table I, we present the expectation values of the lowest resonant states of total angular momentum $L = 0, 1, 2$ found within the Rydberg series converging to the $H^-(1s^2)+e^+$ threshold. In the table, the notation $L^{\rm I}(N)$ represents the Nth resonant state of angular momentum L, and the superscript I indicates that this state is determined by excluding the Ps($1s$) orbital. The OPP method employed in our calculations enables flexible configuration of angular momentum L through the utilization of the global vector $|\boldsymbol{v}|^{2K+L}$. For the determination of the resonant states, we used a basis set composed of 2000 ECGs.

We calculated the expectation values of the distances between the proton and the electron $\langle r_1\rangle$, between the proton and the positron $\langle r_3\rangle$, and between the positron and the electron $\langle r_{13}\rangle$ for the resonant states. These values were then compared with the corresponding expectation values for $H^-(1s^2)$, which were obtained by employing a basis set of 300 ECGs while maintaining the same level of precision. Our analysis demonstrated that the $\langle r_1\rangle$ values for the $S^{\rm I}(1)$, $P^{\rm I}(1)$, and $D^{\rm I}(1)$ states closely matched that of $H^-(1s^2)$, particularly for the D-wave resonant state. This suggests that these states can be interpreted as a positron attaching to $H^-(1s^2)$, with the positron exerting less influence on the inner core of $H^-(1s^2)$ in the higher states.

The OPP basis set incorporates valuable information about the dissociation channels by elevating the OPP energy to a higher level. Consequently, it proves to be an exceptional tool for performing intricate coordinate rotation calculations. By employing the CCR method with the OPP basis, we have successfully identified the resonant states present in the Rydberg series, which converge to $H^-(1s^2)+e^+$ for the S, P, and D symmetry, respectively. These resonant states are presented in Table II and compared with previous findings [19,25]. Our results closely align with these earlier studies, underscoring the reliability of the OPP method based on SVM for computing resonances in the PsH system.

TABLE II. Resonance position E_R (first entry) and width $\Gamma/2$ (second entry) for the S-, P-, and D-wave resonance lying in the Rydberg series converging to the $H^-(1s^2)+e^+$ threshold.

State	Present	Hylleraas	22Ps1H
	−0.602808	−0.60278[a]	−0.5978[b]
$S^I(1)$	0.001764	0.001753	0.0013
	−0.56810	−0.5682[a]	−0.5676[b]
$S^I(2)$	0.00081	0.00092	0.00061
	−0.55262	−0.55248[a]	−0.5520[b]
$S^I(3)$	0.00072	0.0005	0.00059
	−0.592501	−0.59245[c]	−0.5883[b]
$P^I(1)$	0.000793	0.00082	0.0053
	−0.56516	−0.56398[c]	−0.5623[b]
$P^I(2)$	0.00117	0.00104	0.0031
	−0.5558		−0.5498[b]
$P^I(3)$	0.0049		0.0015
	−0.57685	−0.57678[c]	−0.5731[b]
$D^I(1)$	0.00172	0.00178	0.0012
	−0.55628	−0.55611[c]	−0.5574[b]
$D^I(2)$	0.00243	0.00134	0.00165

[a]Ref. [25].
[b]Ref. [19].
[c]Ref. [22].

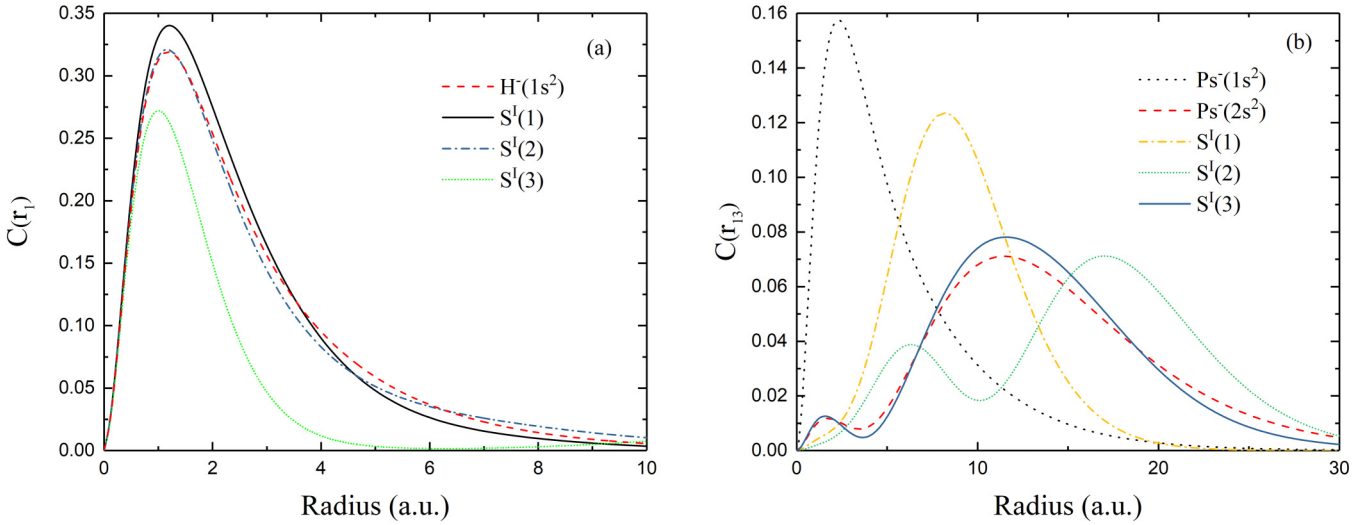

FIG. 2. Probability density distributions of the distances between the proton and electron r_1 (a) and between the positron and electron r_{13} (b) for the lowest S-wave resonant states in the $H^-(1s^2) + e^+$ Rydberg series.

In the OPP method, locating the lowest resonant states is a straightforward process. However, distinguishing higher resonant states from the diagonalized pseudostates can be challenging. The difficulty can be overcome through the application of the complex coordinate rotation method, which allows for efficient differentiation of these resonant states. Moreover, utilizing the OPP basis can provide valuable structural information about higher-order resonant states. By examining the probability density distributions of r_1 and r_{13} for the $S^{\rm I}(1)$, $S^{\rm I}(2)$, and $S^{\rm I}(3)$ states, we can enhance our understanding of the system's configuration. These distributions, also known as the correlation functions, illustrate the density between two charged particles as a function of distance [29].

The probability density distribution of r_{ij} is defined by the following equation:

$$C(r_{ij}) = \int d\Omega_{r_{ij}} r_{ij}^2 \langle \Psi | \delta(\mathbf{b}^T \mathbf{x} - \mathbf{r}_{ij}) | \Psi \rangle, \qquad (10)$$

where the symbol $\langle \ldots \rangle$ represents integration over the relative coordinates and $\int d\Omega_{\mathbf{r}_{ij}}$ denotes integration over the orientation of $\mathbf{r}_{ij}$.

Figure 2 depicts the probability density distributions of r_1 and r_{13} for the three lowest resonant states and $H^-(1s^2)$. All states show a prominent peak at approximately 1.2 a.u. in the probability density distribution of r_1 [see Fig. 2(a)]. However, the probability density distributions of r_{13} reveal the similarity only between the $S^{\rm I}(3)$ state and $Ps^-(2s^2)$ [refer to Fig. 2(b)]. As a result, the probability density distribution effectively demonstrates that the $S^{\rm I}(N)$ configuration resembles a positron attaching to $H^-(1s^2)$. On the other hand, the $S^{\rm I}(3)$ state presents a unique configuration similar to a positron attaching to $H^-(1s^2)$ and a proton attaching to $Ps^-(2s^2)$. These probability density distributions offer valuable insights into the configuration of resonant states and can prove highly valuable in the search for Rydberg series.

B. Resonant states in Rydberg series converging to the $H^-(2s^2) + e^+$ or $Ps^-(1s^2) + H^+$ threshold

In this subsection, we present another OPP calculation involving the utilization of the penalty function $\phi_{\rm H}(\boldsymbol{r})$ to exclude the H(1s) orbital. This action aims to raise the OPP energies, thereby encompassing higher resonant states that may be part of the Rydberg series converging to the $H^-(2s^2) + e^+$ or $Ps^-(1s^2) + H^+$ threshold. This OPP operator can be defined as follows:

$$\hat{P} = |\phi_{\rm H}(\boldsymbol{r}_1)\rangle\langle\phi_{\rm H}(\boldsymbol{r}_1)| + |\phi_{\rm H}(\boldsymbol{r}_2)\rangle\langle\phi_{\rm H}(\boldsymbol{r}_2)|. \qquad (11)$$

In this case, $|\phi_{\rm H}(\boldsymbol{r})\rangle$ represents the wave function of the H(1s) orbital, which is expressed as a linear combination of ten ECGs, resulting in the ground-state energy of $-0.499\,999$ a.u.

It is noted that the calculations presented here are more intricate and time consuming when compared to the previous case of excluding the Ps(1s) orbital. The convergence of expectation values for the resonant states with $L = 0$ is demonstrated in Table III, using a basis set of 6000 ECGs. In this table, the label $S^{\rm II}(N)$ represents the Nth resonant state with $L = 0$, while the superscript II indicates that this state is determined by excluding the H(1s) orbital. In this specific calculation, the OPP energy $E_{\rm OPP}$ converges to at least 10^{-6} a.u., while $\lambda\langle\hat{P}\rangle$ also reaches convergence at 10^{-7} a.u. These convergence criteria provide strong evidence for the precision and reliability of the obtained results. It is worth noting that the OPP calculation for $L = 1$ and 2 involves considerably more complexity, which will require further studies.

The $\langle r_1 \rangle$ value for the $S^{\rm II}(1)$ state is approximately 6.9 a.u., closely matching the $\langle r_1 \rangle$ value of $H^-(2s^2)$ at 7.6 a.u. Conversely, the $\langle r_{13} \rangle$ value for the $S^{\rm II}(1)$ state is approximately 4.6 a.u., which is close to that of $Ps^-(1s^2)$ at 5.4 a.u. This differs from the $S^{\rm I}(1)$ state, where $\langle r_{13} \rangle$ is nearly twice that of $Ps^-(1s^2)$. These results suggest that the $S^{\rm II}(1)$ state could possess a unique configuration, possibly resembling both $H^-(2s^2) + e^+$ and $Ps^-(1s^2) + H^+$.

TABLE III. Convergence of expectation values for the lowest S-wave resonant state $S^{II}(1)$ in the Rydberg series converging to the $H^-(2s^2)+e^+$. Values are given in atomic units.

N	E_{OPP}	$\langle r_1\rangle$	$\langle r_3\rangle$	$\langle r_{13}\rangle$	$\langle r_1^2\rangle$	$\langle r_3^2\rangle$	$\langle r_{13}^2\rangle$	$\langle\delta(\mathbf{r}_1)\rangle$	$\langle\delta(\mathbf{r}_{13})\rangle$
4000	−0.3916619	6.9328	7.8687	4.5855	56.247	69.117	30.044	0.01124	0.02220
4500	−0.3916631	6.9332	7.8702	4.5859	56.257	69.158	30.054	0.01130	0.02220
5000	−0.3916637	6.9334	7.8706	4.5862	56.262	69.170	30.059	0.01129	0.02224
5500	−0.3916641	6.9335	7.8709	4.5863	56.266	69.178	30.062	0.01129	0.02224
6000	−0.3916643	6.9336	7.8711	4.5864	56.268	69.183	30.065	0.01130	0.02224

To extract further structural information, we use the probability density distribution. Figure 3(a) displays the probability density distributions of r_1 for the $S^{II}(N)$ and $H^-(2s^2)$ states. Notably, both the $S^{II}(1)$ and $H^-(2s^2)$ states exhibit strong similarities, each featuring two peaks at positions 1 and 6 a.u., reflecting a typical double-excited state configuration. However, for the $S^{II}(2)$ to $S^{II}(3)$ states, the 6-a.u. peak undergoes substantial distortion, suggesting their deviation from this double-excited state configuration.

Figure 3(b) shows the probability density distributions of r_{13} for the $S^{II}(N)$ and $Ps^-(1s^2)$ states. All $S^{II}(N)$ states exhibit similarity to $Ps^-(1s^2)$, displaying a single peak at the position 2.5 a.u. By considering the r_1 distribution plots, we can deduce that the $S^{II}(2)$ to $S^{II}(4)$ states possess the distinct $Ps^-(1s^2)+H^+$ configuration, placing them within the $Ps^-(1s^2)+H^+$ Rydberg series. However, the classification of the $S^{II}(1)$ state is less straightforward, as it exhibits features indicative of both $H^-(2s^2)+e^+$ and $Ps^-(1s^2)+H^+$ structures, warranting further analysis.

The CCR method, when combined with the OPP basis, offers a refined approach for determining S-wave resonant states. The computed $S^{II}(N)$ resonances are listed in Table IV and can be classified into distinct Rydberg series based on the quantum defect formula [24,25]. In a previous study [25], this formula was used to classify eight states within the $H^-(1s^2)+e^+$ Rydberg series. In the present context, the same classification scheme is employed to assign the $S^{II}(N)$ states to the appropriate Rydberg series. Notably, prior research [14] reported resonances within the $H^-(2s^2)+e^+$ Rydberg series for states $n=2$ to 5 but omitted the $n=1$ state. By using the quantum defect formula, it can be proven that this missing $n=1$ resonant state corresponds to the $S^{II}(1)$ state. The quantum defect formula mentioned above is

$$\Delta E=\frac{1}{2(n-\mu)^2}, \tag{12}$$

where the binding energy ΔE can be computed as $\Delta E=E_R-E_{\text{threshold}}$, where $E_{\text{threshold}}=-0.148\,776\,3$ a.u. for $H^-(2s^2)$ [44]. By using previous results for $n=2$–5 states from Ref. [14] to fit the binding energies of the higher resonant states to the quantum defect formula, we can determine the quantum defect μ from the fitting process, yielding a value of $\mu=-0.432\,15$. The fitted resonant energy for the $n=1$ state in the $H^-(2s^2)+e^+$ Rydberg series is $E_R=-0.3926$ a.u., which slightly differs from the actual calculated resonant energy of the $S^{II}(1)$ state, which is $E_R=-0.391\,103$ a.u.. The actual calculated and fitted results are listed in Table V. As a result, the $S^{II}(1)$ state should be classified as part of the $H^-(2s^2)+e^+$ Rydberg series, which can be identified as the $n=1$ doubly excited state that was omitted in that series [14].

The quantum defect formula enables us to classify the $S^{II}(2)$ to $S^{II}(4)$ states into the $Ps^-(1s^2)+H^+$ Rydberg series. However, a modification to the quantum defect formula is

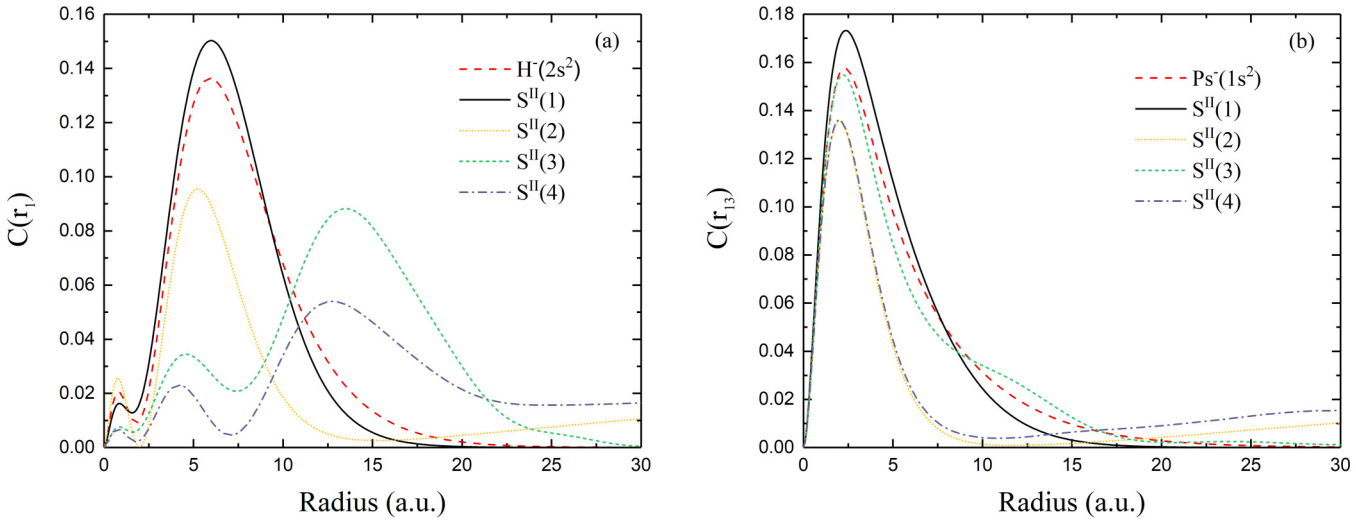

FIG. 3. Probability density distributions of the distances between the proton and electron r_1 (a) and between the positron and electron r_{13} (b) for the lowest S-wave resonant states in the $H^-(2s^2)+e^+$ Rydberg series.

TABLE IV. Resonance position E_R and width $\Gamma/2$ for the S-wave resonances lying in the Rydberg series converging to either the $H^-(2s^2)+e^+$ or the $Ps^-(1s^2)+H^+$ threshold. Values are given in atomic units.

State	Rydberg series	E_R	$\Gamma/2$
$S^{II}(1)$	$H^-(2s^2)+e^+$	−0.391103	0.000606
$S^{II}(2)$	$Ps^-(1s^2)+H^+$	−0.37448	0.00042
$S^{II}(3)$	$Ps^-(1s^2)+H^+$	−0.32078	0.0015
$S^{II}(4)$	$Ps^-(1s^2)+H^+$	−0.30514	0.00063

necessary, presented as follows:

$$\Delta E = \frac{P}{2(n-\mu)^2}, \tag{13}$$

where both the quantum defect μ and the constant P are determined through a fitting process. The binding energies $\Delta E = E_R - E_{\text{threshold}}$, where $E_{\text{threshold}} = -0.262\,005\,07$ a.u., applicable for $Ps^-(1s^2)$ [45]. We conduct a fitting of the binding energies to this modified quantum defect formula, based on previous results of $n = 4$ to 6 states derived from Ref. [24]. This fitting yields values of $P = 2.400$ and $\mu = -2.365$. It is important to highlight that the current fitting procedure differs significantly from that explained in the previous work [24]. A comparison of these two fitting procedures is presented in Fig. 4. The results of the present fitting demonstrate a significantly reduced fitting error. The difference can be primarily attributed to the fact that the $n = 1$ and 2 states (referred to as $1S$ and $2S$) in Ref. [24] cannot be classified within the $Ps^-(1s^2)+H^+$ Rydberg series. In Ref. [24], the $1S$ state corresponds to the present $S^I(3)$ state, both of which exhibit nearly identical resonant positions: $E_r = -0.552\,62$ a.u. for the $S^{II}(3)$ state and $E_r = -0.5531$ a.u. for the $1S$ state. Similarly, the $2S$ state in Ref. [24] corresponds to the current $S^{II}(1)$ state. These states also have similar resonant positions: $E_r = -0.391\,103$ a.u. for the $S^{II}(1)$ state and $E_R = -0.391\,09$ a.u. for the $2S$ state. The distinct configuration of the $S^I(3)$ and $S^{II}(1)$ states accounts for this reclassification. The probability density distributions of these two states reveal a unique configuration that can be described as an e^+ attached to H^- as well as an H^+ attached to Ps^-. The recommended Rydberg series converging to the $H^-(2s^2)+e^+$ and $Ps^-(1s^2)+H^+$ are classified in Table V, which includes both the calculated and fitted results.

TABLE V. Resonances in PsH lying in the Rydberg series converging to the $H^-(2s^2)+e^+$ and $Ps^-(1s^2)+H^+$ thresholds. The fitted results are obtained using the quantum defect formulas Eqs. (12) and (13) for the third and fifth column, respectively.

	$H^-(2s^2)+e^+$		$Ps^-(1s^2)+H^+$	
n	E_R	Fitted	E_R	Fitted
1	−0.391103[a]	−0.3926	−0.37448[a]	−0.3680
2	−0.2317[b]	−0.2333	−0.32078[a]	−0.3250
3	−0.1941[b]	−0.1912	−0.30514[a]	−0.3037
4	−0.1767[b]	−0.1742	−0.2916[c]	−0.2916
5	−0.1679[b]	−0.1657	−0.2842[c]	−0.2841
6			−0.2791[c]	−0.2791
∞	−0.1488		−0.2620	

[a]Present.
[b]Ref. [14].
[c]Ref. [24].

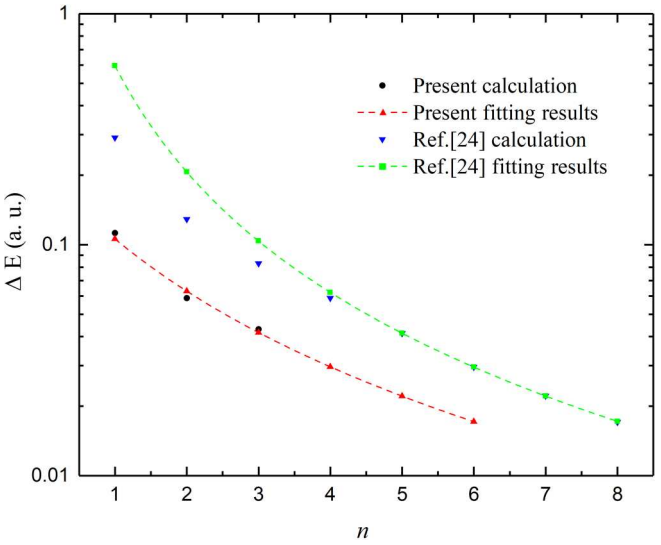

FIG. 4. Comparison of the current quantum defect formula Eq. (13) with the previous fitting. The binding energy ΔE is measured relative to the threshold of $Ps^-(1s^2)$ and n is the principal quantum number.

IV. CONCLUSION

We have conducted an extensive investigation of autodissociating resonant states in PsH, which exhibit a doubly excited nature. To achieve this, we utilized a combination of the projection operator method and the SVM. The OPP method, in conjunction with the CCR method, was employed to identify resonant states situated below the $H^-(1s^2)+e^+$ threshold, as well as those below the $H^-(2s^2)+e^+$ and $Ps^-(1s^2)+H^+$ thresholds in particular. Moreover, the OPP basis played a pivotal role in unveiling the structural attributes of these resonant states.

Through a comprehensive analysis that incorporated probability density distribution and the quantum defect formula, we successfully clarified and refined two Rydberg series that converge to the $H^-(2s^2)+e^+$ and $Ps^-(1s^2)+H^+$ thresholds. Notably, we confirmed the existence of a unique configuration within the $S^I(3)$ and $S^{II}(1)$ states, where an e^+ is attached to H^- and an H^+ is attached to Ps^-. This configuration highlights the distinctive nature of these two states, particularly in the context of scattering phenomena involving excited H and Ps.

The insights gained from this paper are expected to make valuable contributions to the experimental investigation of resonances in Ps-H scattering and optical transitions.

ACKNOWLEDGMENTS

This work was supported by the National Natural Science Foundation of China under Grants No. 12364059, No. 12274106, No. 12174399, and No. 11934014, and by the

Natural Science Foundation of Hainan Province under Grants No. 122QN219 and No. 122MS005. Z.C.Y. was supported by the Natural Sciences and Engineering Research Council of Canada.

[1] A. Dalgarno and R. A. McCray, Astrophys. J. **181**, 95 (1973).
[2] P. J. Sarre, J. Chim. Phys. **77**, 769 (1980).
[3] T. J. Millar, C. Walsh, and T. A. Field, Chem. Rev. **117**, 1765 (2017).
[4] G. Weidenspointner, G. Skinner, P. Jean, J. Knödlseder, P. von Ballmoos, G. Bignami, R. Diehl, A. W. Strong, B. Cordier, S. Schanne, and C. Winkler, Nature (London) **451**, 159 (2008).
[5] R. Laha, Phys. Rev. Lett. **123**, 251101 (2019).
[6] D. M. Schrader, F. M. Jacobsen, N.-P. Frandsen, and U. Mikkelsen, Phys. Rev. Lett. **69**, 57 (1992).
[7] J. Usukura, K. Varga, and Y. Suzuki, Phys. Rev. A **58**, 1918 (1998).
[8] Z.-C. Yan and Y. K. Ho, Phys. Rev. A **59**, 2697 (1999).
[9] J. Mitroy, Phys. Rev. A **73**, 054502 (2006).
[10] M. W. J. Bromley, J. Mitroy, and K. Varga, Phys. Rev. A **75**, 062505 (2007).
[11] T. Yamashita, E. Hiyama, D. Yoshida, and M. Tachikawa, Phys. Rev. A **105**, 012814 (2022).
[12] R. J. Drachman and S. K. Houston, Phys. Rev. A **12**, 885 (1975).
[13] R. J. Drachman, Phys. Rev. A **19**, 1900 (1979).
[14] Y. K. Ho, Phys. Rev. A **41**, 68 (1990).
[15] C. P. Campbell, M. T. McAlinden, F. G. R. S. MacDonald, and H. R. J. Walters, Phys. Rev. Lett. **80**, 5097 (1998).
[16] Z.-C. Yan and Y. K. Ho, Phys. Rev. A **57**, R2270 (1998).
[17] Y. K. Ho and Z.-C. Yan, J. Phys. B **31**, L877 (1998).
[18] Y. K. Ho and Z.-C. Yan, Phys. Rev. A **62**, 052503 (2000).
[19] J. E. Blackwood, M. T. McAlinden, and H. R. J. Walters, Phys. Rev. A **65**, 030502(R) (2002).
[20] J. Di Rienzi and R. J. Drachman, Phys. Rev. A **65**, 032721 (2002).
[21] J. DiRienzi and R. J. Drachman, Phys. Rev. A **66**, 054702 (2002).
[22] Z.-C. Yan and Y. K. Ho, J. Phys. B **36**, 4417 (2003).
[23] J. DiRienzi and R. J. Drachman, Phys. Rev. A **76**, 032705 (2007).
[24] Z.-C. Yan and Y. K. Ho, Phys. Rev. A **78**, 012711 (2008).
[25] Z.-C. Yan and Y. K. Ho, Phys. Rev. A **84**, 034503 (2011).
[26] K. Varga and Y. Suzuki, Phys. Rev. C **52**, 2885 (1995).
[27] G. G. Ryzhikh, J. Mitroy, and K. Varga, J. Phys. B **31**, 3965 (1998).
[28] J. Mitroy, S. Bubin, W. Horiuchi, Y. Suzuki, L. Adamowicz, W. Cencek, K. Szalewicz, J. Komasa, D. Blume, and K. Varga, Rev. Mod. Phys. **85**, 693 (2013).
[29] Y. Suzuki, M. Suzuki, and K. Varga, *Stochastic Variational Approach to Quantum-Mechanical Few-Body Problems* (Springer Science & Business Media Springer, New York, 1998), Vol. 54.
[30] M. W. J. Bromley, J. Mitroy, and K. Varga, Phys. Rev. Lett. **109**, 063201 (2012).
[31] J. Mitroy and J. Grineviciute, Phys. Rev. A **88**, 022710 (2013).
[32] Y. Zhang, M.-S. Wu, Y. Qian, K. Varga, H.-L. Han, and J.-Y. Zhang, Phys. Rev. A **102**, 012825 (2020).
[33] V. M. Krasnopolskij and V. I. Kukulin, Yad. Fiz. **20**, 883 (1974).
[34] A. K. Bhatia, A. Temkin, and J. F. Perkins, Phys. Rev. **153**, 177 (1967).
[35] A. K. Bhatia and A. Temkin, Phys. Rev. A **11**, 2018 (1975).
[36] J. Mitroy and G. Ryzhikh, Comput. Phys. Commun. **123**, 103 (1999).
[37] S. Bubin, M. Pavanello, W.-C. Tung, K. L. Sharkey, and L. Adamowicz, Chem. Rev. **113**, 36 (2013).
[38] M.-S. Wu, J.-Y. Zhang, Y. Qian, K. Varga, U. Schwingenschlögl, and Z.-C. Yan, Phys. Rev. A **103**, 022817 (2021).
[39] T. F. O'Malley and S. Geltman, Phys. Rev. **137**, A1344 (1965).
[40] W. P. Reinhardt, Annu. Rev. Phys. Chem. **33**, 223 (1982).
[41] Y. Ho, Phys. Rep. **99**, 1 (1983).
[42] V. I. Korobov, Phys. Rev. A **67**, 062501 (2003).
[43] V. I. Korobov, Phys. Rev. A **89**, 014501 (2014).
[44] L. G. Jiao and Y. K. Ho, Phys. Rev. A **87**, 052508 (2013).
[45] Y. K. Ho, Phys. Rev. A **48**, 4780 (1993).